JOURNAL OF SOLID STATE CHEMISTRY **125,** 91–101 (1996)
ARTICLE NO. 0269

New Mixed Valence Compounds in the Pb–V–O System: Synthesis and Crystal Structure of Hollandite-Related $Pb_{1.32}V_{8.35}O_{16.7}$ and *R*-Type Hexagonal Ferrite PbV_6O_{11}

O. Mentre and F. Abraham[1]

Laboratoire de Cristallochimie et Physicochimie du Solide URA CNRS 452 ENSCL, Université des Sciences et Technologies de Lille, BP 108, 59652 Villeneuve d'Ascq Cedex, France

Received February 7, 1996; in revised form May 13, 1996; accepted May 15, 1996

Two new mixed valence vanadium oxides $Pb_{1.32}V_{8.35}O_{16.7}$ and PbV_6O_{11} have been discovered in the Pb–V–O system. Their crystal structures were determined at room temperature by single-crystal X-ray analysis. $Pb_{1.32}V_{8.35}O_{16.7}$: monoclinic, $I2/m$, $a = 10.108(3)$, $b = 9.887(3)$, $c = 2.903(1)$ Å, $\gamma = 90.84(2)°$, and $Z = 1$, final $R = 0.049$ for 452 independent refections. PbV_6O_{11}: hexagonal, $P6_3mc$, $a = 5.754(1)$, $c = 13.267(3)$ Å and $Z = 2$, final $R = 0.035$ for 353 independent reflections. For $Pb_{1.32}V_{8.35}O_{16.7}$, V(1) and V(2) octahedra form a hollandite-type framework. Pb(1) and Pb(2) alternate randomly with O(5) atoms in the hollandite-type tunnels which are fully occupied. The O(5) atoms create additional oxygen tetrahedra occupied by intratunnel V(3) atoms. The structure of PbV_6O_{11} is closely related to $BaTi_2Fe_4O_{11}$ and AV_6O_{11} compounds (A = Na, Sr) which adopt an *R*-type hexagonal ferrite structure: O and Pb atoms form a hexagonal close-packed structure, and V(1), V(2), and V(3) atoms are surrounded octahedrally by six oxygen atoms. $V(2)O_6$ and $V(3)O_6$ octahedra are face-shared and occupied by V^{3+} and V^{4+} ions, respectively, whereas they are equivalent in other AV_6O_{11} compounds. The lack of symmetry due to the lone pair effect of the Pb^{2+} ion is responsible for the split of these vanadium atoms. The Pb^{2+} ion is displaced from the center of the cuboctahedron to a basal O_3 triangle and forms an umbrella-like PbO_3 entity. As a consequence, the V(4) atom is also off-centered in the trigonal-bipyramid and its environment is rather better described as a tetrahedron, like Fe^{3+} in numerous magnetoplumbite-type compounds.

INTRODUCTION

Numerous studies have been done on oxides with the general formula $A_xM_8O_{16}$ ($x \leqslant 2$) that crystallize with the same structure as the minerals hollandite, cryptomelane, and priderite (tetragonal or monoclinic pseudo-tetragonal symmetry). The smaller M cation may be a combination of two metals or one metal present at two different oxidation states (Mn, V, Cr, Ti, Ru, Mo). The A cation may be monovalent (Na, K, Rb, Cs, Tl, Ag) or divalent (Ba, Pb) (1–4) and occupies the large tunnels of the M_8P_{16} host lattice. Recently the synthesis and structure of the hollandite-type oxide $La_{1.16}Mo_8O_{16}$ in which the tunnel cations are trivalent have been reported (5). In a recent paper we described the preparation and the crystal structure of the first Bismuth hollandite-type compound obtained with mixed valency vanadium as the M cation: $Bi_{1.62}V_8O_{16}$ (6). The existence of previously reported high pressure–high temperature synthesized $Tl_{1.74}V_8O_{16}$ (7) led us to expect such an $A_xV_8O_{16}$ material with $A = Pb^{2+} - 6s^2$ lone pair cation.

Attempts to prepare $Pb_2V_8O_{16}$ led to needle-shaped and black hexagonal-platelet single crystals. We report in this paper the crystal structure determination of these two kinds of single crystals that correspond to two stoichiometrically closely related oxides.

EXPERIMENTAL

Synthesis

In hollandite oxides the tunnel sites may be fully ($A_2M_8O_{16}$ compounds) or partially occupied. The occupancy of the large tunnels by the lead cations of a hypothetic $Pb_xV_8O_{16}$ compound being, of course, unknown, the $Pb_2V_8O_{16}$ composition has been arbitrarily chosen for the synthesis. A mixture of PbO, V_2O_3, and V_2O_5 corresponding to the reaction

$$2PbO + 3V_2O_3 + V_2O_5 \rightarrow Pb_2V_8O_{16}$$

was first heated at 850°C for 96 hr in a silica tube sealed under primary vaccum. At this stage, X-ray powder analysis of the product revealed a monoclinic, deformed, hollandite-type compound as the primary phasis. The powder

[1] To whom correspondence should be addressed.

0022-4596/96 $18.00

sample was then reheated in a sealed, evacuated silica tube at 1200°C for 48 hr to grow single crystals of this doubtful hollandite phase. The product thus obtained was not homogeneous, but composed of black needles and hexagonal-platelet single crystals accompanied by black powder. EDS (energy dispersive spectroscopy) microprobe elemental analysis was performed on a Philips 525M scanning electron microscope connected to an Edax PV9900 analyzer and revealed V : Pb ratios close to 6 : 1 for the two kinds of single crystals.

To determine the actual composition of the two different single crystals, they were investigated by X-ray diffraction.

Structure Determinations

(*a*) $Pb_{1.32}V_{8.35}O_{16.7}$. A black needle was mounted with the greatest dimension of the needle as the rotation axis. Oscillation and Weissenberg photographs indicated $2/m$ Laue symmetry. Systematic absences (hkl: $h + k = 2n + 1$) were consistent with space groups $C2$, Cm, and $C2/m$. The preliminary cell parameters were $a = 14.10$, $b = 2.90$, $c = 9.90$ Å, and $\beta = 134.2°$ corresponding to a distorted hollandite framework. This cell is in fact equivalent to the nonconventional body-centered monoclinic framework with **c** as the binary axis and unit cell parameters $a = 10.10$, $b = 9.90$, $c = 2.90$ Å, and $\gamma = 90.62°$. This orientation was chosen for the data collection to allow an easier comparison with the ideal tetragonal hollandite-type material structures. Single crystal X-ray diffraction data were collected on a Philips PW1100 automated diffractometer under the conditions given in Table 1. The intensity of each reflection was corrected for background and for Lorentz and polarization effects. The absorption corrections were performed using the analytical method of De Meulenaer and Tompa (8) with, for the first stages of the determination, a linear absorption coefficient calculated for a hypothetical formula $Pb_2V_8O_{16}$ and with the true value after the actual formula had been determined.

The structure refinement has been achieved in the nonconventional $I112/m$ space group. Correlation between standard $I4/m$ and $I112/m$ coordinates is given by

$I4/m$		$I112/m$
	→	$8j$ x, y, z
$16i$ x, y, z		
	→	$8j$ y, x, z.

An approximated two vanadium and four oxygen independent atom skeleton based on the Bi-hollandite structural study (6) was first introduced in the refinement process leading to the high reliability factor $R = 0.34$ and $R_w = 0.41$.

A subsequent Fourier difference synthesis showed a lead atom in a $4(g)$ site $(0, 0, z)$ with $z = 0.24$ and a refined occupancy of 0.26. At this stage U_{ij} anisotropic thermal factors were refined for Pb and V atoms leading to $R = 0.11$ and $R_w = 0.13$. In the following difference map, a maximum was observed with coordinates $x = 0.04$, $y = 0$, $z = 1/2$. It was first fixed at a $2(b)$ $(0, 0, 1/2)$ site, but residual electronic peaks on the $z = 1/2$ plane split it so that the $4(i)$ $(x, y, 1/2)$ special position seemed to be indicated. Distance considerations suggest a lead atom in this site according to the prismatic environment with four Pb–O distances close to 2.7 Å. The site occupation factor refined to $\tau = 0.12$ sets $R = 0.07$ and $R_w = 0.08$. A subsequent Fourier difference map revealed a last maximum at $4(i)$ $(x, y, 0)$ with $x = 0.98$ and $y = 0.12$. The residual peak was assigned to vanadium atoms occupying the host channels of the hollandite framework with a low refined occupancy of $\tau = 0.09$ and $B = 1.17$ Å^2 ($R = 0.061$, $R_w = 0.064$).

The chemical formula deduced from the structure study is $Pb_{1.32}V_{8.35}O_{16}$. In the last cycles of refinement, U_{ij} thermal parameters were introduced for the two last added atoms. Refinement of a secondary extinction coefficient and the introduction of a weighting scheme gave the results reported in Table 2 ($R = 0.049$, $R_w = 0.052$). Bond distances and bond angles for the environment of cations are given in Table 3.

(*b*) PbV_6O_{11}. A black hexagonal plate shaped crystal was isolated from the preparation and mounted on a glass fiber. Its shape is in agreement with the hexagonal unit cell ($a = 5.75$, $c = 13.27$ Å), Laue symmetry $6/mmm$, found after a preliminary oscillation and Weissenberg study. Absences of hhl reflections are consistent with space groups $P6_3mc$, $P6_3/mmc$, and $P\bar{6}2c$, however the structure refinements were performed satisfactorily only in the noncentrosymmetric $P6_3mc$ space group leading to fully occupied atomic positions and acute reliability factors. Refinement attempts in other space groups are discussed in the following section. Half of the reciprocal space was recorded with a CAD-4 Enraf Nonius automated diffractometer with the data reported in Table 1. Absorption corrections were first performed according to the method of De Meulenaer and Tompa (8) considering an approximated absorption coefficient $\mu = 250$ cm^{-1}.

Calculation of the Patterson function showed that lead atoms are located in the $2(b)$ special position of the $P6_3/mmc$ space group. A Fourier difference synthesis calculated with $|F_{obs}| - |F_{Pb}|$ allowed the location of vanadium atoms in $6(g)$, $4(e)$ ($z \sim 0.15$), and $2(d)$ special positions. Refinement led to abnormally high temperature factors for vanadium atoms and high reliability factor (≈0.29), preventing oxygen maxima from appearing at the subsequent Fourier difference maps. The same difficulties were encountered in the $P\bar{6}2c$ space group for which vanadium atoms occupy the same special positions with $x \sim 0.5$ for the $6(g)$ position. In the $P6_3mc$ space group, vanadium atoms are located in the equivalent special positions: $6(c)$

TABLE 1
Crystal Data, Intensity Measurement, and Structure Refinement Parameters for the Two Studied Single Crystals

	$Pb_{1.32}V_{8.35}O_{16.7}$	PbV_6O_{11}
	Crystal data	
Crystal symmetry	Monoclinic	hexagonal
Space group	$I2/m$	$P6_3mc$
Cell dimension (Å)	$a = 10.108(3)$, $b = 9.887(3)$ $C = 2.903(1)$, $\gamma = 90.84(3)$	$a = 5.754(1)$, $c = 13.267(3)$
Volume (Å^3)	290.37	380.4
Z	1	2
	Data collection	
Equipment	Philips PW 1100	Nonius CAD 4
λ (Mo$K\alpha$ (graphite monochromotor))	0.7107 Å	0.7107 Å
Scan mode	ω-2Θ	ω-2Θ
Scan width (°)	1.2	0.8 + 0.34 tan Θ
Θ range (°)	2–35	2–35
Standard reflections measured every 2 hr (no decay)	310, 060, 030	110, 022, 120
Recording reciprocal space	$-16 \le h \le 16$, $-13 \le k \le 13$, $0 \le l \le 4$	$-9 \le h \le 9$, $-9 \le k \le 9$, $0 \le l \le 21$
Number of measured reflections	1380	3554
Number of reflections $I > 3\sigma(I)$	857	2936
Number of independent reflections	452	353
μ(cm^{-1}) (for λ $K\alpha$ = 0.7107 Å)	256.5	293.7
Limiting faces and distances(mm) from an arbitrary origin	100 $\bar{1}00$ 0.017 $0\bar{1}0$ 010 0.015 001 $00\bar{1}$ 0.062	001 $00\bar{1}$ 0.028 010 $0\bar{1}0$ 0.108 100 0.07 $\bar{1}00$ 0.075 $1\bar{1}10$ 0.07 $\bar{1}10$ 0.066
Transmission factor range	0.37–0.49	0.04–0.21
Merging R factor	0.035	0.053
	Refinement	
Number of refined parameters	46	32
$R = \Sigma \lvert F_o - F_c \rvert / \Sigma \lvert F_o \rvert$	0.049	0.035
$R_w = [\Sigma w (\lvert F_o \rvert - \lvert F_c \rvert)^2 / \Sigma w F_o^2]^{1/2}$ With $w = 1/\sigma(F_o)$	0.052	0.036

(with $x \sim 0.5$ and $z \sim 0.0$) $\equiv 6(g)$, $2(a)$ (with $z \sim 0.15$) + $2(a)$ (with $z \sim 0.35$) $\equiv 4(e)$, and $2(b)$ (with $z \sim 0.25$) $\equiv 2(d)$. Refinement of these positions and isotropic thermal factors led to reliability factors $R = 0.098$ and $R_w = 0.117$ and acceptable B displacement parameters (the z coordinate of Pb was first set at $z = 1/4$ to fix the origin along the **c**-axis). A subsequent Fourier difference synthesis showed five independent oxygen atoms in two kinds of special positions: $6(c)$ (x, x, z) for O(1), O(2), and O(3) and $2(b)$ (2/3, 1/3, z) for O(4) and O(5) leading to the PbV_6O_{11} chemical formula. At this stage, the z coordinate of O(2) was fixed at $z = 3/4$ as the origin to allow an easier comparison with isostructural compounds. That shifted the Pb atom from $z = 1/4$ to the $z = 0.230(1)$ refined value. In the last cycles of refinement, anisotropic displacement factors for Pb and V atoms were refined, the actual absorption coefficient $\mu = 293.7$ cm^{-1} was used, secondary extinction was taken into account, and a weighting scheme was introduced yielding $R = 0.038$, $R_w = 0.040$. Since the structure is not centrosymmetric, changing the enantiomorphic specification by reversing the sign of the imaginary part of anomalous dispersion yields the final values $R = 0.035$ and $R_w = 0.036$ and allows one to set up the absolute configuration of the true structure. The atomic parameters with isotropic and anisotropic temperature factors are presented in Table 4. Table 5 shows the important distances and angles in PbV_6O_{11}.

For the two structure determinations, the atomic scattering factors for neutral atoms were taken from the "International Tables for X-ray Crystallography" (9) and values for the anomalous dispersion corrections were taken from Cromer and Liberman (10). The full matrix least-squares refinements were performed with a local modification of the SFLS-5 program (11).

TABLE 2
Positional Parameters and Coefficients of the Anisotropic Thermal Factors for $Pb_{1.32}V_{8.35}O_{16}$

Atom	Site	Occ.	Positional parameters x	y	z	B or B_{eq} (Å^2)[a]
Pb(1)	4*g*	0.208(5)	0	0	0.230(1)	1.92(6)
Pb(2)	4*i*	0.122(5)	0.530(1)	0.484(1)	0	8.0(5)
V(1)	4*i*	1	0.3538(1)	0.1700(1)	0	0.62(3)
V(2)	4*i*	1	0.8325(1)	0.3519(1)	0	0.67(3)
V(3)	4*i*	0.087(7)	0.9836(17)	0.123(2)	0	0.8(4)
O(1)	4*i*	1	0.1569(5)	0.1945(6)	0	0.63(9)
O(2)	4*i*	1	0.8002(5)	0.1518(6)	0	0.87(9)
O(3)	4*i*	1	0.5393(6)	0.1739(6)	0	0.87(9)
O(4)	4*i*	1	0.8413(5)	0.5390(6)	0	0.67(9)

Atom	Anisotropic temperature coefficients[b] U_{11}	U_{22}	U_{33}	U_{12}	U_{13}	U_{23}
Pb(1)	0.0367(17)	0.025(1)	0.010(1)	0.0009(8)	0	0
Pb(2)	0.11(1)	0.109(8)	0.08(1)	0.073(6)	0	0
V(1)	0.0099(6)	0.0078(6)	0.0061(6)	0.0006(4)	0	0
V(2)	0.0104(7)	0.0099(7)	0.0051(6)	−0.0017(5)	0	0
V(3)	0.008(8)	0.02(1)	0.001(7)	−0.006(6)	0	0

[a] The B_{eq} are defined by $B_{eq} = 4/3 \sum i \sum j \beta_{ij} a_i a_j$.
[b] The anisotropic temperature factor is defined by $U = \exp(-2\pi^2[\sum_i \sum_j h_i h_j a_i^* a_j^* U_{ij}])$.

From the structure studies the compositions of the two single crystals are $Pb_{1.32}V_{8.35}O_{16}$ and PbV_6O_{11}. However, for the first compound, from crystal-chemical considerations discussed below, a further oxygen atom must be added so that the composition of the phase must be $Pb_{1.32}V_{8.35}O_{16.70}$. Attempts to synthesize the title compounds in a pure form, by reacting PbO, V_2O_5, and V_2O_3 in stoichiometric ratios, failed. Most of the experiments led to a mixture of the two phases in approximatively equal proportions, whatever the initial composition and reaction temperature. The best results were obtained when mixtures were heated in a flattened and sealed gold tube at 800°C for 48 hr: PbV_6O_{11} was admixed by a small quantity of the hollandite related phase and $Pb_{1.32}V_{8.35}O_{16.7}$ by a small amount of an unidentified phase (Fig. 1). The powder patterns showed in Fig. 1 were obtained with a Siemens D5000 diffractometer (Cu$K\alpha$ radiation) equipped with a diffracted beam, graphite crystal monochromator. The unit cell parameters were refined using data provided by these patterns (Tables 6 and 7). The peak intensities observed on diffraction patterns are compared with the intensity of powder diffraction lines calculated from the program LAZY-PULVERIX (12) based on single crystal structure results. It is obvious that the observed intensities are affected by preferred orientation.

DISCUSSION

In $Pb_{1.32}V_{8.35}O_{16.70}$, V(1) and V(2) octahedra form a $[V_8O_{16}]$ framework analogous to those of hollandite (1). The symmetry of ideal hollandite compounds is tetragonal as in priderite, however for numerous compounds the structure distorts and the symmetry is lowered from tetragonal to monoclinic as in the mineral hollandite itself (1). However, the classical $[M_8O_{16}]$ framework is kept although slightly distorted. It consists of infinite rutile chains parallel to the **c**-axis sharing edges to form double strings. V(1) and V(2) double strings are connected at their corners to form a $[V_8O_{16}]$ framework structure containing rutile-type channels (1 × 1 octahedra) along [001] and large tunnels (2 × 2 octahedra) with a square cross section. One of the most interesting aspects of the hollandite structure is occupancy of the large tunnels. In $Pb_{1.32}V_{8.35}O_{16.70}$, they are occupied by Pb(1), Pb(2), and V(3) atoms (Fig. 2).

Byström and Byström (13) placed the tunnel cations of their ideal hollandite at the 2(*b*) special position defined by the intersection of the mirror plane and axis of the

TABLE 3
Interatomic Distances (Å) and Angles (°) for $Pb_{1.32}V_{8.35}O_{16.7}$

V(1) environment	
	2 × O(3)–V(1)–O(1) : 92.9(4)
	2 × O(3)–V(1)–O(4) : 93.9(4)
1 × V(1)–O(1) : 2.008(5)	1 × O(3)–V(1)–O(4) : 172(4)
2 × V(1)–O(1) : 1.979(4)	1 × O(4)–V(1)–O(4) : 96.3(2)
1 × V(1)–O(3) : 1.875(6)	2 × O(4)–V(1)–O(1) : 91.4(3)
2 × V(1)–O(4) : 1.947(4)	2 × O(4)–V(1)–O(1) : 84.3(3)
⟨V(1)–O⟩ = 1.956	2 × O(4)–V(1)–O(1) : 173(3)
	2 × O(1)–V(1)–O(1) : 81.6(3)
	1 × O(1)–V(1)–O(1) : 94.3(2)
V(2) environment	
	2 × O(4)–V(2)–O(2) : 92.3(3)
	2 × O(4)–V(2)–O(3) : 96.2(4)
1 × V(2)–O(2) : 2.000(6)	1 × O(4)–V(2)–O(2) : 173(4)
2 × V(2)–O(2) : 1.976(3)	1 × O(3)–V(2)–O(3) : 95.2(2)
2 × V(2)–O(3) : 1.964(4)	2 × O(3)–V(2)–O(2) : 88.3(3)
1 × V(2)–O(4) : 1.851(6)	2 × O(3)–V(2)–O(2) : 84.5(3)
⟨V–O⟩ = 1.955	2 × O(3)–V(2)–O(2) : 171(2)
	2 × O(2)–V(2)–O(2) : 83.1(4)
	1 × O(2)–V(2)–O(2) : 94.5(1)
V(3) environment	
1 × V(3)–O(1) : 1.88(1)	1 × O(1)–V(3)–O(2) : 149(2)
1 × V(3)–O(2) : 1.87(1)	1 × O(5)–V(3)–O(5) : 99.3(6)
2 × V(3)–O(5) : 1.90(1)	2 × O(5)–V(3)–O(1) : 98.4(6)
⟨V(3)–O⟩ = 1.88	2 × O(5)–V(3)–O(2) : 101.3(7)
Pb(1) environment	
2 × Pb(1)–O(1) : 2.563(5)	1 × O(1)–Pb(1)–O(1) : 150(1)
2 × Pb(1)–O(2) : 2.620(5)	1 × O(2)–Pb(1)–O(2) : 150(16)
⟨Pb(1)–O⟩ = 2.581	2 × O(1)–Pb(1)–O(2) : 88.7(3)
	2 × O(1)–Pb(1)–O(2) : 83.6(3)
Pb(2) environment	
2 × Pb(2)–O(1) : 2.83(1)	1 × O(1)–Pb(2)–O(1) : 61.7(1)
2 × Pb(2)–O(2) : 2.63(1)	1 × O(2)–Pb(2)–O(2) : 66.9(2)
⟨Pb(2)–O⟩ = 2.73	2 × O(1)–Pb(2)–O(2) : 111(4)
	2 × O(1)–Pb(2)–O(2) : 78.5(3)

TABLE 4
Positional Parameters and Coefficients of the Anisotropic Thermal Factors for PbV_6O_{11}

Atom	Site	Occ.	Positional parameters x	y	z	B or B_{eq} (Å^2)[a]
Pb	2*b*	1	1/3	2/3	0.2231(6)	0.78(1)
V(1)	6*c*	1	0.5112(2)	−0.5112(2)	−0.0021(6)	0.28(3)
V(2)	2*a*	1	0	0	0.1447(7)	0.30(6)
V(3)	2*a*	1	0	0	0.3501(7)	0.26(6)
V(4)	2*b*	1	2/3	1/3	0.2633(7)	0.43(7)
O(1)	6*c*	1	0.1764(9)	−0.1764(9)	0.0776(9)	0.28(12)
O(2)	6*c*	1	0.1516(10)	−0.1516(10)	3/4	0.43(13)
O(3)	6*c*	1	0.1713(8)	−0.1713(8)	0.4169(9)	0.19(11)
O(4)	2*b*	1	2/3	1/3	0.4109(15)	0.55(24)
O(5)	2*b*	1	2/3	1/3	0.0936(14)	0.43(23)

Atom	Anisotropic temperature coefficients[b] U_{11}	U_{22}	U_{33}	U_{12}	U_{13}	U_{23}
Pb	0.0080(2)	$= U_{11}$	0.00106(3)	$= U_{11}/2$	0	0
V(1)	0.0021(4)	$= U_{11}$	0.00049(6)	0.0004(5)	0.0001(1)	$= -U_{13}$
V(2)	0.0027(7)	$= U_{11}$	0.0005(2)	$= U_{11}/2$	0	0
V(3)	0.0023(7)	$= U_{11}$	0.0004(1)	$= U_{11}/2$	0	0
V(4)	0.0026(8)	$= U_{11}$	0.0010(2)	$= U_{11}/2$	0	0

[a] The B_{eq} are defined by $B_{eq} = 4/3 \sum i \sum j \beta_{ij} a_i a_j$.
[b] The anisotropic temperature factor is defined by $U = \exp(-2\pi^2[\sum_i \sum_j h_i h_j a_i^* a_j^* U_{ij}])$.

*I*4/*m* tetragonal space group. Then cations are coordinated by eight equivalent oxygen atoms at the vertices of a tetragonal prism. In fact, cations are often displaced from the 2(*b*) Wyckoff position to a more stable one, which is approximatively located at the distance of the nearest oxygen atoms equal to the sum of the ionic radii (1). For instance, in $Bi_{1.62}V_8O_{16}$, Bi^{3+} is displaced from the 2(*b*) to the 4(*e*) position (0, 0, *z*) with $z = 0.10$ leading to a practically square planar coordination with four Bi–O distances of 2.473 Å and an O–Bi–O angle of 166°. Pb(1) atoms occupy, in our case, a 4(*g*) site (0, 0, *z*) with $z = 0.23$ and so is displaced nearer to the **c**-axis origin than in the mineral hollandite. Pb(1) is at the top of a PbO_4 pyramid with two Pb(1)–O(1) distances of 2.56 Å and two Pb(1)–O(2) distances of 2.62 Å. This kind of lead pyramidal environment is commonly found. For example, in red PbO lead oxide (14), Pb atoms are at the top of a PbO_4 pyramid with four Pb–O distances of 2.32 Å and two O–Pb(1)–O angles of 118°. The hollandite $Pb(1)O_4$ pyramid is flatter with two angles of 150°. In fact, the coordination around Pb(1) must be completed by the Pb^{2+}stereoactive lone pair; the oxygen atoms and the lone pair form a square pyramid centered by the Pb atom. Galy and Enjalbert reported that the center Es of the sphere of influence of the Pb^{2+} lone pair is at 0.86 Å from the Pb^{2+} cation center (15). On the basis of their results Es occupies, in the Pb–V hollandite, a (0, 0, *z*) position with $z = 0.52$ which is very close to the 2(*b*) cationic site of the ideal *I*4/*m* hollandite.

Pb(2) and V(3) atoms are both offset in the tunnels. The Pb(2) atom is shifted from the 2(*b*) site, not along the [001] direction of the tunnel but in the (001) plane to become the nearest neighbor of two O(1) and two O(2) atoms. Pb (2) atoms are thus at the top of a square pyramid $Pb(2)O(1)_2O(2)_2$, less flat than $Pb(1)O_4$. The Pb(2)–O(1) and Pb(2)–O(2) distances are, respectively, 2.63(1) and 2.83(1) Å and the O(1)–Pb(2)–O(2) angle is 111(4)°. The O_4 basal plane of the pyramid is parallel to the **c**-axis and extends over two unit cells. The Pb(2) atom is about 0.7 Å from the Pb(2)′ ($x = 0.470$, $y = 0.516$, $z = 0$) equivalent position by the twofold axis. Thus, the two related positions cannot be simultaneously occupied. For the reasons mentioned above the center Es of the sphere of influence of the Pb^{2+} lone pair is located near the Pb(2)′ position. Pb(2) atoms are so randomly distributed over Pb(2) and Pb(2)′ sites.

Intratunnel V(3) atoms are coordinated to one O(1) and one O(2) atom of the channels edges with an O(1)–V(3)–O(2) angle of 149(2)°. This coordination of the V(3) atom is quite unusual and unlikely. It may be completed to a tetrahedral coordination by two missing O(5) atoms which

TABLE 5
Interatomic Distances (Å) and Angles (°) for PbV_6O_{11}

V(1) environment	
	1 × O(1)–V(1)–O(1) : 86.1(5)
	1 × O(3)–V(1)–O(3) : 93.9(4)
2 × V(1)–O(1) : 1.983(9)	1 × O(4)–V(1)–O(5) : 174(6)
2 × V(1)–O(3) : 1.913(9)	2 × O(1)–V(1)–O(4) : 82.6(6)
1 × V(1)–O(4) : 2.114(9)	2 × O(1)–V(1)–O(5) : 84.8(2)
1 × V(1)–O(5) : 1.998(10)	2 × O(1)–V(1)–O(3) : 173(5)
⟨V–O⟩ = 1.984	2 × O(1)–V(1)–O(3) : 89.6(7)
	2 × O(3)–V(1)–O(4) : 91.1(4)
V(2) environment	
3 × V(2)–O(1) : 1.971(9)	3 × O(1)–V(2)–O(1) : 101.2(7)
3 × V(2)–O(2) : 2.053(8)	3 × O(2)–V(2)–O(2) : 78.8(3)
⟨V–O⟩ : 2.012	3 × O(1)–V(2)–O(2) : 164(3)
	6 × O(1)–V(2)–O(2) : 88.9(5)
	2 × O(3)–V(2)–O(5) : 93.1(7)
V(3) environment	
3 × V(3)–O(2) : 2.007(8)	3 × O(2)–V(3)–O(2) : 81.0(3)
3 × V(3)–O(3) : 1.924(9)	3 × O(3)–V(3)–O(3) : 100.4(4)
⟨V–O⟩ = 1.965	3 × O(2)–V(3)–O(3) : 166(3)
	6 × O(2)–V(3)–O(3) : 88.4(6)
V(4) environment	
3 × V(4)–O(2) : 1.826(7)	3 × O(2)–V(4)–O(2) : 119.1(6)
1 × V(4)–O(4) : 1.960(16)	1 × O(4)–V(4)–O(5) : 180(16)
1 × V(4)–O(5) : 2.259(16)	3 × O(4)–V(4)–O(2) : 95.5(8)
⟨V–O⟩ = 1.939	3 × O(5)–V(4)–O(2) : 84.4(6)
Pb–O distances	
3 × Pb–O(1) : 2.485(12)	
6 × Pb–O(2) : 2.903(4)	
3 × Pb–O(3) : 3.036(13)	
⟨Pb–O⟩ = 2.831	

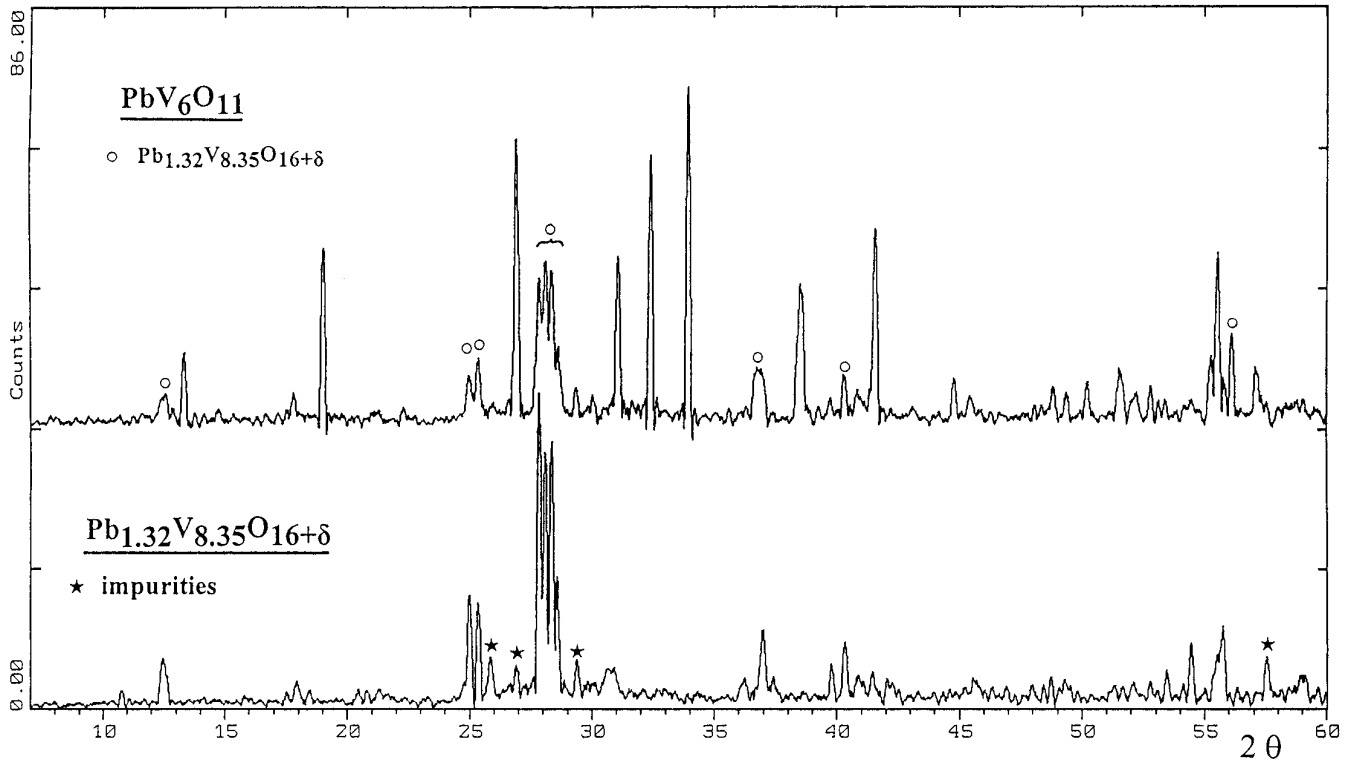

FIG. 1. X-ray powder diffraction patterns of PbV_6O_{11} and $Pb_{1.32}V_{8.35}O_{16.7}$.

should be located in the 2(*b*) site at the center of the tunnels. Because of their proximity to the Pb(2) sites, introduction of these hypothetical O(5) atoms in the refinement process is not realistic. Such O(5) located atoms are present in $A_{2-x}V_{8+2x}O_{16+x}$ (16, 17) and in the recently published $BaV_{10-x}O_{14}$ (18) pseudo-hollandite phases. In these compounds, they complete an octahedral V(3)–O(5) atom coordination with an acceptable V(3) distance of 1.80 Å in $BaV_{9.89}O_{17}$ (18). Figure 3 allows a comparison between tetrahedral and octahedral intratunnel vanadium atoms. In our case, the tetrahedral V(3)–O(5) distance (1.90(1) Å) is close to V(3)–O(1) and V(3)–O(2) distances, however $V(3)O_4$ tetrahedra are highly distorted considering the large O(1)–V(3)–O(2) angle of 149°. The V–O distance suggest that the V(3) site is occupied by a V^{3+} cation. The bond valence sum calculation using data of Brown and Altermatt (19) confirms this hypothesis (Table 8). In all the hollandite-related vanadium oxides, this calculation indicates that V(1) and V(2) sites are occupied by both V^{3+} and V^{4+}; the bond valence sums for these sites are close for our Pb-hollandite and $K_2V_8O_{16}$ in accordance with the values of the mean oxidation state of V atoms. In $A_{2-x}V_{8+2x}O_{16+x}$ (A = K, Rb) the O(5) atom must bond to two adjacent V(3) atoms to be stable, because a monovalent neighboring A cation cannot provide sufficient electrostatic force to the O(5) atom. V(3)–V(3) distances presented by Abriel *et al.* for $K_{0.78}V_{10.44}O_{17.22}$, $K_{0.92}V_{10.16}O_{17.08}$, and $Rb_{0.9}V_{10.2}O_{17.1}$ compounds are, respectively, 3.63, 3.64, and 3.61 Å (17). In $BaV_{10-x}O_{17}$, on the other hand, a divalent Ba cation provides a strong enough electrosatic force to the O(5) atom so the two adjacent available V(3) sites are not always both occupied. A $BaV_{9.89}O_{17}$ single crystal study revealed a V(3)–V(3) distance of 3.60 Å. In our case, the occupancy of two neighboring V(3) sites related by the twofold axis leads to two $V(3)O_4$ tetrahedra linked by an O(5)–O(5) edge with a V(3)–V(3) distance of 2.47 Å which is highly improbable. $V(3)O_4$ tetrahedra could also be linked by O(5) corners to form finite or infinite zig-zag chains parallel to the **c**-axis. A more satisfactory hypothesis is a random distribution of Pb(1), Pb(2), and $V(3)O_4$ tetrahedra within the large tunnels. When the sites are occupied in two consecutive unit cells by two O(5) atoms (of one $V(3)O_4$ tetrahedron), the occupancy of the two neighboring cells by Pb(1) atoms (Fig. 4) leads to a Pb(1)–O(5) distance of 2.12 Å which is an acceptable value. Thus the postulated O(5) atom is bonded to V(3) and to Pb(1) atoms which provide sufficient electrostatic force to the O(5) atom.

Hollandite-related compounds exhibit two available host sites per unit cell. Occupancies of the three independent entities present in the tunnels imply that a tunnel is randomly occupied by 0.832 Pb(1), 0.488 Pb(2), and 0.7

TABLE 6
Observed and Calculated X-Ray Powder Diffraction Pattern for $Pb_{1.32}V_{8.35}O_{16.7}$ from Siemens D5000 Goniometer Data (λ = 1.54056 Å)

h k l	$2\theta_{obs}$	$2\theta_{calc}$	I_{obs}/I_o	I_{calc}/I_o
$\bar{1}$ 1 0	12.424	12.421	16.1	16.5
1 1 0	12.604	12.605	14.9	19.7
2 0 0	—	17.534	—	1.5
0 2 0	—	17.929	—	0.1
$\bar{2}$ 2 0	25.005	24.992	26.1	34.6
2 2 0	25.364	25.367	34.0	37.5
3 1 0	27.845	27.826	100	100
$\bar{3}$ 1 0	28.086	28.082	71.2	51.3
1 3 0	28.344	28.338	69.0	42.7
$\bar{1}$ 3 0	28.567	28.589	31.3	93.2
1 0 1	—	32.066	—	0.4
0 1 1	—	32.123	—	0.7
4 0 0	—	35.496	—	1.5
0 4 0	—	36.317	—	1.2
$\bar{2}$ 1 1	36.763	36.760	7.5	19.2
2 1 1	—	36.893	—	24.8
$\bar{1}$ 2 1	36.904	36.911	13.5	25.8
1 2 1	37.023	37.043	8.9	17.4
$\bar{3}$ 3 0	—	37.877	—	0.1
3 3 0	—	38.458	—	0.1
$\bar{4}$ 2 0	39.766	39.791	8.5	12.0
4 2 0	40.286	40.288	13.6	12.3
$\bar{2}$ 4 0	40.367	40.353	11.7	9.8
2 4 0	40.863	40.843	10.0	15.9
3 0 1	—	41.017	—	18.1
0 3 1	41.448	41.428	8.9	22.6

Note. Refined parameters: $a = 10.108(3)$ Å, $b = 9.887(3)$ Å, $c = 2.903(1)$ Å, $\gamma = 90.84(2)°$.

O(5) (meaning 0.35 V(3)O_4 tetrahedra). The average occupancy per unit cell is 0.832 + 0.488 + 0.7 = 2.02 leading to fully occupied tunnels. It is noteworthy that in other hollandite-related vanadium oxides, $BaV_{10-x}O_{17}$ (18) and $A_{2-x}V_{8+2x}O_{16+x}$ (16, 17), the tunnels are also fully occupied. Thus the actual composition of this phase is closely related to $Pb_{1.32}V_{8.35}O_{16.7}$.

Despite the composition closeness to $Pb_{4/3}V_{8+1/3}O_{16+2/3}$, propitious to tunnel hosts arrangement, neither intratunnel nor intertunnel ordering has been detected by oscillation and Weissenberg photographs.

PbV_6O_{11} is essentially isostructural with $BaTi_2Fe_4O_{11}$ (20–22), $BaSn_2Fe_4O_{11}$ (22, 23), $BaFe_2Ru_4O_{11}$ (24), and MV_6O_{11} (M = Na, Sr) (25–30) compounds. Their structures are closely related to $BaFe_{12}O_{19}$ (31, 32), a well known hexagonal ferrite having a magnetoplumbite structure. The structure of $BaFe_{12}O_{19}$ can be described as the packing along the **c**-axis of the hexagonal cell of so-called R blocks $(Ba^{2+}Fe_6^{3+}O_{11})^{2-}$, and S spinel blocks, $(Fe^{3+}O_8)^{2+}$, following the RSR^*S^* sequence (the * symbol denotes that the same block has been turned 180° around the **c**-axis). R blocks in RR^* structure were first isolated by the $BaTi_2Fe_4O_{11}$ synthesis, Ti^{4+} introduction bringing electroneutrality to the R-block (20). More recently electroneutrality has been obtained with mixed valency vanadium in NaV_6O_{11} synthesized for the first time by electrolytic reduction of molten $NaVO_3$ (25). NaV_6O_{11} was also obtained by solid state reaction (26). Lately SrV_6O_{11} and $SrT_xV_{6-x}O_{11}$ (T = Ti, $0 < x \leq 1.5$, T = Cr, $0 < x \leq 1.0$, T = Fe, $0 < x \leq 1.4$) were synthesized (27). PbV_6O_{11} is the first R-type hexagonal ferrite compound containing lead. R and R^* blocks of PbV_6O_{11} are shown in Fig. 5.

The structure of PbV_6O_{11} can be described by the stacking along the **c**-axis of four O_4 and two PbO_3 layers according to the following sequence: –(PbO_3)–(O_4)–(O_4)– with a hexagonal close packing. V(1), V(2), and V(3) atoms occupy the octahedral sites while the V(4) atom is near the center of a triangular bipyramid whose triangular basal plane is formed by three oxygen atoms of the PbO_3 layers (Fig. 6).

All the published results assign the centrosymetric

TABLE 7
Observed and Calculated X-Ray Powder Diffraction Pattern for PbV_6O_{11} from Siemens D5000 Goniometer Data (λ = 1.54056 Å)

h k l	$2\theta_{obs}$(°)	$2\theta_{calc}$(°)	I_{obs}/I_o	I_{calc}/I_o
0 0 2	13.334	13.336	16.9	17
1 0 0	17.786	17.782	6.9	9.2
1 0 1	19.010	19.006	51.8	50.4
1 0 2	22.270	22.292	3.6	4.9
0 0 4	26.860	26.857	47.4	23.3
1 0 3	26.924	26.931	40.6	39.0
1 1 0	31.061	31.055	46.6	55.2
1 0 4	32.397	32.396	69.4	61.6
1 1 2	33.936	33.932	100	100
2 0 0	—	36.011	—	0.8
2 0 1	36.666	36.664	11.1	10.6
1 0 5	38.405	38.400	24.1	18.0
2 0 2	38.564	38.562	36.6	40.4
0 0 6	—	40.776	—	2.3
1 1 4	41.406	41.512	7.3	9.5
2 0 3	41.567	41.563	62.1	43.6
1 0 6	44.799	44.803	12.9	5.4
2 0 4	—	45.489	—	1.9
2 1 0	—	48.273	—	1.6
2 1 1	48.828	48.790	8.5	11.2
2 0 5	50.170	50.180	12.9	9.1
2 1 2	—	50.311	—	1.8
1 0 7	51.535	51.545	20.6	15.1
1 1 6	—	51.121	—	8.1
2 1 3	—	52.778	—	7.4
3 0 0	55.238	55.249	16.8	9.7
0 0 8	—	55.349	—	3.2
2 0 6	56.105	55.514	46.1	33.3

Note. Refined parameters: $a = 5.754(1)$ Å, $c = 13.267(3)$ Å.

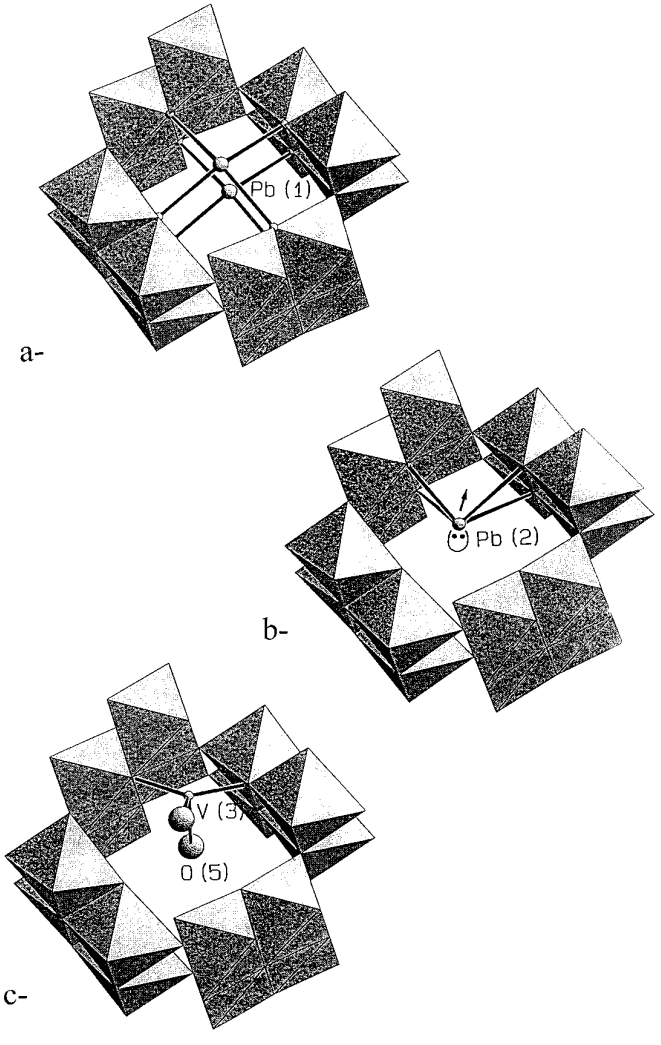

FIG. 2. Coordination of (a) Pb(1), (b) Pb(2), and (c) V(3) within the tunnels of the hollandite $Pb_{1.32}V_{8.35}O_{16.7}$.

TABLE 8
Bond Valence in Four Hollandite Related Oxides

Site	V(1)		V(2)		V(3)		Mean oxidation state for vanadium
Assumed valence	+3	+4	+3	+4	+3	+4	
$BaV_{9.89}O_{17}$	+3.18	+3.46	+3.03	+3.38	+2.76	+3.09	3.24
$K_{0.78}V_{10.44}O_{17.22}$	+3.12	+3.48	+2.92	+3.26	+2.74	+3.06	3.22
$Pb_{1.32}V_{8.35}O_{16.7}$	+3.40	+3.80	+3.41	+3.81	+2.75	+3.03	3.68
$K_2V_8O_{16}$	+3.40	+3.80	+3.40	+3.80			3.75

$P6_3/mmc$ space group to the hexagonal *R*-type ferrites at room temperature (20–22). NaV_6O_{11} was first reported to crystallize in $P\bar{6}2c$ (25), but Kanke *et al.* described it later in the $P6_3/mmc$ space group (29). Similar results were found for other mixed valency vanadium oxides, e.g., SrV_6O_{11} or substituted $SrT_xV_{6-x}O_{11}$ (T = Ti, Cr, Fe) whose structures were solved by Rietveld analysis of their neutron powder diffraction data (27). The existence of mirror symmetry at $z = 1/4$ in $P6_3/mmc$ and $P\bar{6}2c$ space groups would place the Pb atom on the O(2) plane resulting in a symmetrical coordination polyhedron. As in hollandite-type compounds, the Pb atom is displaced from the center of its polyhedron toward the O(1) plane, leading to three shorter Pb–O(1) distances of 2.485 (12) Å. Actually, Pb is at the center of a PbO_3E tetrahedron, formed by three O(1) atoms and completed by the lone pair E of Pb^{2+} which is oriented toward the O(3) triangle (Fig. 7). In PbV_6O_{11} the steric effect of the $6s^2$ lone pair of Pb^{2+} is probably the main reason for the space group asymmetry. In the $P6_3/mmc$ space group, Pb atoms should be split over two positions on both sides of the mirror (4(*f*) Wyckoff position) with half occupancy; refinement of such a model did not converge.

NaV_6O_{11} undergoes a two-step second-order structural

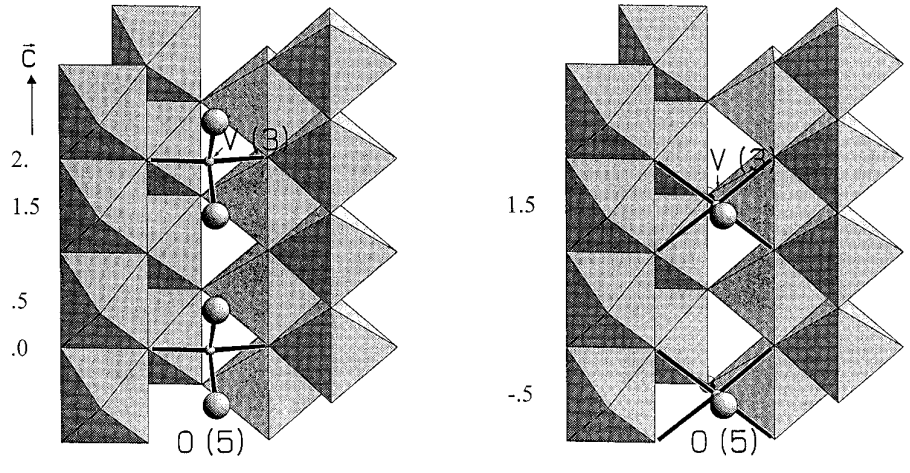

FIG. 3. Comparison between tetrahedral and octahedral vanadium in the tunnels of the hollandige-related vanadium oxides (z values for V and O(5) atoms are given on the **c**-axis).

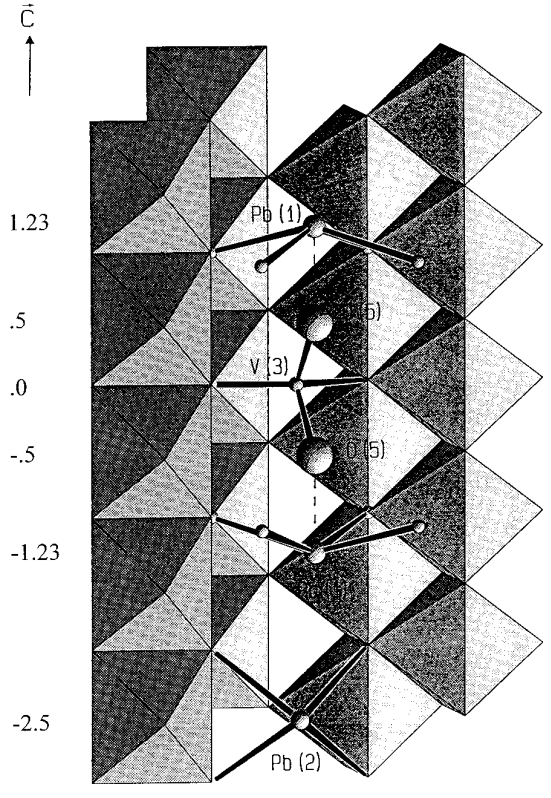

FIG. 4. Possible O(5) environment in lead–vanadium hollandite (z values for intratunnel ions are given on the **c**-axis).

phase transition upon cooling: hexagonal ($P6_3/mmc$) → hexagonal ($P6_3mc$) → orthorhombic ($Cmc2_1$) at, respectively, 245 and 35–40 K (30). X-ray single crystal data refinement at 200 K showed that NaV_6O_{11} is essentially isostructural with PbV_6O_{11}, as a consequence of the lack of the center of symmetry but, in our case, the asymmetry is emphasized. Pb and V(4) triangular bipyramidal atoms are on both sides of the pseudo-mirror containing the O(2) atoms with the splits $\Delta = 0.35$ Å (Pb) and $\Delta = 0.17$ Å (V(4)) greater than in the $P6_3mc$ NaV_6O_{11} state ($\Delta = 0.03$ Å for Na, $\Delta = 0.063$ Å for V). Some other differences between these two isostructural compounds concerned the distortion of the vanadium polyhedra. The $V(1)O_6$ octahedron is more distorted in PbV_6O_{11} with O–V–O bond angles spanning a 82.6°–93.9° range. The V(1) atom deviates from the plane composed of the equatorial O(1) and O(3) atoms to elongate the apical V(1)–O(4) distance (2.114 Å) and shortens the opposite V(2)–O(5) distance (1.998 Å). Moreover an additional distortion appears in the equatorial basis, V(1)–O(1) distances (1.983(9) Å) being much longer than V(1)–O(3) (1.913(9) Å).

$V(2)O_6$ and $V(3)O_6$ octahedra share an oxygen $O(2)_3$ face to form dimeric units which connect the V(1) octahedral sheets. These two octahedra are equivalent in R-type compounds adopting $P6_3/mmc$ symmetry; they are highly distorted. The three V–O(2) distances with common oxygen atoms are elongated whereas the other vanadium oxygen distances are shortened and the O(2)–V–O(2) angles are acute relaxing V–V Coulomb repulsion. In NaV_6O_{11}

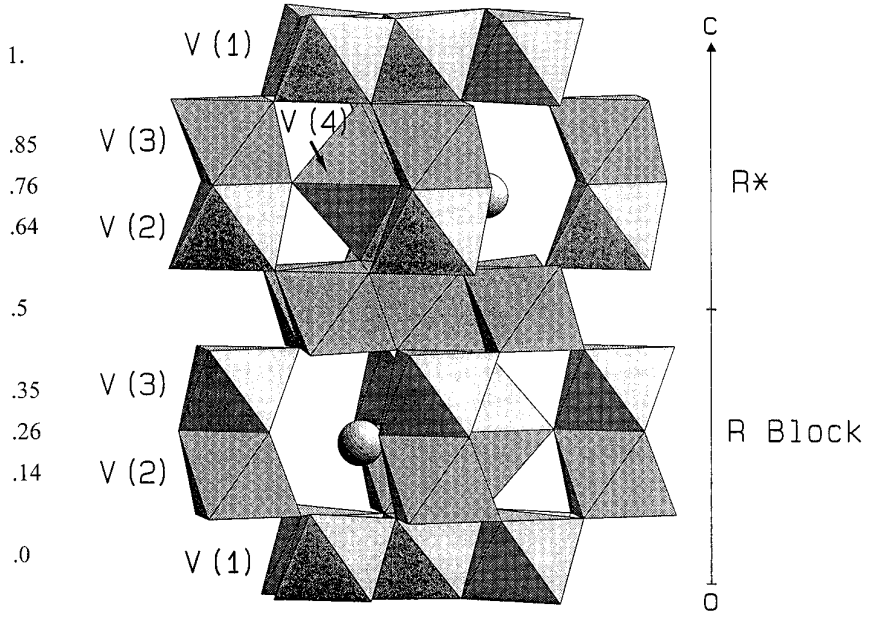

FIG. 5. Crystal structure of PbV_6O_{11}. V(1), V(2), and V(3) atoms form octahedra whereas the V(4) atom is displaced from the center of a trigonal-bipyramid site. Pb is also displaced from the center of a cuboctahedron.

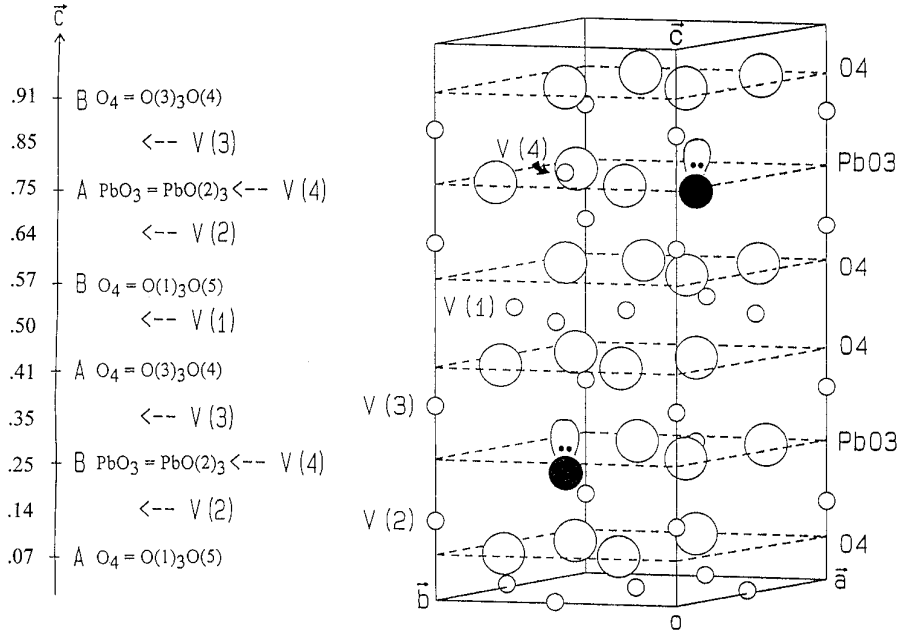

FIG. 6. Stacking sequences of layers along the **c**-axis in PbV_6O_{11}.

at 200 K ($P6_3mc$ space group), the V(2)O_6 octahedra of a dimer split into two nonequivalent VO_6 octahedra, however the V–O distances remain almost unchanged. In contrast, in PbV_6O_{11}, the two octahedra become very different: for the V(3) atom the V–O distances are close to those in NaV_6O_{11}, and for the V(2) atom all the V–O distances are about 0.05 Å longer. The V–V distance across the shared octahedral face is elongated (2.725 Å in PbV_6O_{11} compared to 2.68 Å in both forms of NaV_6O_{11}).

The location of the trigonal-bipyramidal cations in the *R* block compounds has been extensively discussed because of its dynamic characteristics and its high thermal ellipsoids in the **c** direction. Consequently this bipyramid could be regarded as two tetrahedra sharing a face in the $P6_3/mmc$ mirror plane. In 1974, Haberey *et al.* presented an ideal model for $BaFe_4Ti_2O_{11}$ in which the centers of the bipyramidal sites were occupied by cations (20). Then, Obradors proposed for $BaFe_{12}O_{19}$ three hypotheses about this site occupancy (32). In the first, the trigonal bipyramidal site is occupied by the Fe^{3+} cations with a root mean square thermal amplitude of 0.22 Å along the **c**-axis. The second, already proposed by Obradors *et al.* (21) and by Cadee *et al.* (22), assumes the existence of a static disorder of the cations on the two pseudo-tetrahedral sites of the bipyramid. The last presented a dynamic disorder of the cations which would move from one site to the other. Structural and Mössbauer features allowed them to select the last model.

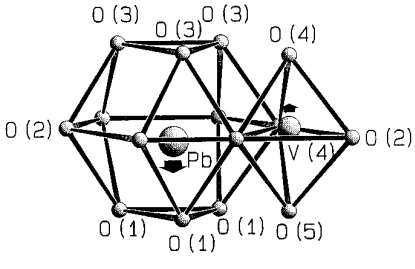

FIG. 7. Opposite Pb and V(4) displacements from the O(2) plane.

The V(4) position is refined 0.17 Å above the triangular base of the bipyramid with the normal isotropic temperature factor $B_{eq} = 0.57$ Å^2. No residual electronic peak was apparent on the other side on a final Fourier difference synthesis. Thus we can conclude that, as in other vanadium compounds, V(4) atoms are not split. Vanadium is five-coordinated with three short basal V–O distances (1.826 Å) and two longer apical distances of 1.960 and 2.259 Å. However the difference between these two V–O distances is much greater than in other MV_6O_{11} compounds leading to a rather fourfold coordination of vanadium atoms rarely found for V^{3+} or V^{4+}, but certainly seen for V(3) in the hollandite $Pb_{1.32}V_{8.35}O_{16.7}$.

The stability ad electroneutrality of PbV_6O_{11} is assured by the simultaneous presence of trivalent and tetravalent vanadium atoms whose relative distribution over the sites has been studied for other $A(T, V)_6O_{11}$ compounds. Electrostatic site potentials and Madelung energies were calculated for several compounds (27, 29) but don't point out a general simple rule, results depending on the nature of the *A* and the *T* atoms. Moreover, these calculations were

TABLE 9
Bond Valence in PbV_6O_{11}

Assumed valence	V(1)	V(2)	V(3)	V(4)
+3	**3.06**	**2.90**	3.36	3.51
+4	3.42	3.24	**3.75**	**3.91**

sometimes in conflict with experimental neutron diffraction data (27). The Brown bond valency method was applied to the PbV_6O_{11} compound, taking account of the V–O distances reported in Table 5. For each V site, the valence was calculated on the basis of a V^{4+} and V^{3+} hypothesis (Table 9). Results suggest V^{3+} for V(1) and V(2) and V^{4+} for V(3) and V(4).

In all the *R* and the *RS*-type hexagonal ferrite compounds studied to date, the *M*(1) site, which corresponds to V(1) in PbV_1O_{11} and to the center of octahedra shared by edges to form layers perpendicular to **c**-axis, are occupied by trivalent cations. Kanke *et al.* (29) concluded that the *M*(3) sites (trigonal-bipyramid) of the AT_6O_{11}-type compounds are preferred by trivalent cations in the case of a divalent *A* ion and by tetravalent cations in the case of a monovalent *A* ion (Table 10). Our results indicate that V(4) sites are in fact favored by V^{4+} despite the divalent Pb ion. The *M*(2) sites (which occupied the face-shared octahedra) split in two nonequivalent V(2) and V(3) sites; bond valence calculations suggest that the V(2) site is occupied by V^{3+} whereas the V(3) site is favored by the V^{4+} ion. Actually, because of its 0.35 Å shift below the $z = 1/4$ pseudo-mirror plane, Pb atoms are nearer to V(2) (Pb–V(2) = 3.459 Å) than V(3) atoms (Pb–V(3) = 3.759 Å). The consequent asymetric electrostatic repulsion in the *R* blocks favors cation V(2) trivalent. Indeed the mean V(2)–O distance, 2.012 Å, agrees with $r(^{VI}V^{3+}) + r(^{IV}O^{2-})$ = 2.02 Åand the mean V(3)–O distance, 1.965 Å, agrees with$r(^{VI}V^{4+}) + r(^{IV}O^{2-})$ = 1.96 Å (33).

As described before, attempts to prepare pure PbV_6O_{11} powder failed. Nor could sufficiently large single crystals be obtained in our preparations. As soon as this problem is solved, magnetic and electric measurements will be investigated to determine PbV_6O_{11} behavior which would reflect the charge distribution of vanadium ions. On the other hand, partial substitution of iron for vanadium allows the preparation of pure $PbV_{6-x}Fe_xO_{11}$ compounds whose structure and properties are under investigation.

TABLE 10
Charge Distribution among *M*(1), *M*(2), and *M*(3) Sites in AV_6O_{11} Compounds with *R*-Type Structure (*A* = Na, Sr, Pb)

Site	NaV_6O_{11}	SrV_6O_{11}	PbV_6O_{11}	Atom in PbV_6O_{11}
M(1)	+3	+3	+3	V(1)
M(2)	+4	+4	+3	V(2)
			+4	V(3)
M(3)	+4	+3	+4	V(4)

REFERENCES

1. J. E. Post, R. B. Von Dreele, and P. R. Buseck, *Acta Crystallogr. B* **38,** 1056 (1982).
2. L. A. Bursill, *Acta. Crystallogr. B* **35,** 530 (1979).
3. V. B. Nalbandyan, I. N. Belyaev, T. G. Lupeiko, and N. V. Mezhzhorina, *Russ. J. Inorg. Chem. (Engl. Trans.)* **24,** 1546 (1979).
4. N. Kinomura, *J. Am. Ceramic Soc.* **56**(6), 344 (1973).
5. H. Leligny, Ph. Labbe, M. Le Desert, and B. Raveau, *Acta Crystallogr. B* **48,** 134 (1950).
6. F. Abraham and O. Mentre, *J. Solid State Chem.* **109,** 127 (1994).
7. W. Abriel, F. Rau, and K. J. Range, *Mater. Res. Bull.* **14,** 1463 (1979).
8. J. De Meulenaer and H. Tompa, *Acta Crystallogr.* **19,** 1014 (1965).
9. "International Tables for X-Ray Crystallography," Vol. IV. Kynoch Press, Birmingham, 1974.
10. D. T. Cromer and D. Liberman, *J. Chem. Phys.* **53,** 1891 (1970).
11. C. T. Prewitt, "SFLS-5, Report ORNL-TM 305." Oak Ridge National Laboratory, Oak Ridge, Tennessee, 1966.
12. K. Yvon, W. Jeitschko, and E. Parthe, *J. Appl. Crystallogr.* **10,** 73 (1977).
13. A. Byström and A. M. Byström, *Acta Crystallogr.* **3,** 146 (1950).
14. R. W. G. Wyckoff (Ed.), "Crystal Structure," Vol. 1, p. 134. Interscience, New York, 1963.
15. J. Galy and R. Enjalbert, *J. Solid State Chem.* **44,** 1 (1982).
16. M. E. De Roy, J. P. Besse, and R. Chevalier, *Mater. Res. Bull.* **21,** 567 (1986).
17. W. Abriel, C. Garbe, F. Rau, and K. J. Range, *Z. Kristallogr.* **176**(1–2), 113 (1986).
18. Y. Kanke, E. Takayama-Muromachi, K. Kato, and K. Kosude, *J. Solid State Chem.* **113,** 125 (1994).
19. I. D. Brown and D. Altermatt, *Acta Crystallogr. B* **41,** 244 (1985).
20. F. Haberey and M. Velicescu, *Acta Crystallogr. B* **30,** 127 (1974).
21. X. Obradors, A. Collomb, J. Pannetier, A. Isalgue, J. Teyada, and J. C. Joubert, *Mater. Res. Bull.* **18,** 1543 (1983).
22. M. C. Cadee and D. J. W. Ijdo, *J. Solid State Chem.* **52,** 171 (1985).
23. M. C. Cadee and D. J. W. Ijdo, *J. Solid State Chem.* **36,** 314 (1981).
24. D. Verdoes, H. W. Zandbergen, and D. J. W. Ijdo, *Mater. Res. Rull.* **22,** 1 (1987).
25. M. E. De Roy, J. P. Besse, and R. Chevalier, *J. Solid State Chem.* **67,** 185 (1987).
26. Y. Kanke, E. Takayama-Muromachi, K. Kato, and Y. Matsui, *J. Solid State Chem.* **89,** 130 (1990).
27. Y. Kanke, F. Izumi, E. Takayama-Muromachi, K. Kato, T. Kamiyama, and H. Asano, *J. Solid State Chem,* **92,** 261 (1991).
28. Y. Uchida, Y. Kanke, E. Takayama-Muromachi, and K. Kato, *J. Phys. Soc. Jpn.* **60,** 2530 (1991).
29. Y. Kanke, K. Kato, E. Takayama-Muromachi, and M. Isobe, *Acta Crystallogr. C* **48,** 1376 (1992).
30. Y. Kanke, F. Izumi, Y. Morii, E. Akiba, S. Funahashi, K. Kato, M. Isobe, E. Takayama-Muromachi, and Y. Uchida, *J. Solid State Chem.* **112,** 429 (1994).
31. W. D. Townes, J. H. Fang, and A. J. Perotta, *Z. Kristallogr.* **125,** 437 (1967).
32. X. Obradors, A. Collomb, M. Pernet, D. Samaras, and J. C. Joubert, *J. Solid State Chem.* **56,** 171 (1985).
33. R. D. Shannon, *Acta Crystallogr. A* **32,** 751 (1976).